Electrochemical behaviour of dissolved iron chloride in KCl+LiCl+NaCl melt at 550ºC

Babak Khalaghi[b,*], Eirin Kvalheim[b], Manabu Tokushige[c], Geir Martin Haarberg[b], Lidong Teng[a], Seshadri Seetharaman[a]

[a] Department of Materials Science and Engineering, Royal Institute of Technology, SE 100 44, Stockholm, Sweden

[b] Department of Materials Science and Engineering, Norwegian University of Science and Technology, NO 7491, Trondheim, Norway

[c] Department of Fundamental Energy Science, Kyoto University, Kyoto 606-8501, JAPAN

Abstract

An electrochemical study of iron was carried out in KCl+LiCl+NaCl melt at 550ºC using a glassy carbon working electrode. Cyclic voltammetry showed that the Fe (II)/Fe (0) electron exchange is a soluble/insoluble reversible process. Chronoamperometry studies suggested that the nucleation of metallic iron on glassy carbon electrode is instantaneous. The diffusion coefficient of Fe (II) was calculated using cyclic voltammetry; 1.4×10^{-5} cm^2 s^{-1}. For the Fe (II)/Fe (III) red/ox reaction, analysis of the voltammograms suggests

* Corresponding author at: Department of Materials Science and Engineering, Royal Institute of Technology (KTH), Brinellvägen 23, SE 100 44, Stockholm, Sweden. Tel.: +46 8 7909089;
E-mail addresses: khalaghi@kth.se (B. Khalaghi), eirin.kvalheim@material.ntnu.no (E. Kvalheim), m-tokushige@saci.kyoto-u.ac.jp (M. Tokushige), lidong@kth.se (L. Teng), raman@kth.se (S. Seetharaman), geir.martin.haarberg@ntnu.no (G.M. Haarberg)

that the process is not reversible and is coupled with a chemical reaction. The stability of $FeCl_3$ and the effect of equilibrium between $FeCl_3$ and $FeCl_2$ are also briefly discussed.

Keywords:

Chloride melts, $FeCl_3$, cyclic voltammetry

1. Introduction

Knowing the electrochemical behaviour of metallic ions in molten salts is crucial for electrometallurgical processes [1,2]. These processes include both extraction of metals from primary sources and recovery from wastes. Recently there has been a growing interest in developing an electrolytic process for iron production [2-5]. Furthermore, while an electrolytic process is used for treatment of wastes, iron is quite often present. Therefore, the electrochemical behaviour of iron in fused salts has been extensively studied. These studies have been performed using different salt mixtures and substrate materials at different temperatures. Some of these electrolytes include KCl+LiCl [6-10], NaCl+KCl [11-13], $ZnCl_2$+2NaCl [14,15], $MgCl_2$+NaCl+KCl [16], $AlCl_3$+NaCl [17], and NaCl [18].

Platinum has shown high reactivity towards iron ions; when it is used as substrate, alloying occurs and the Fe (II) reduction is far from reversible [6,12,16]. Other substrates such as tungsten, glassy carbon and molybdenum have shown inertness towards iron ions [6,11,13-17] with one exception for tungsten [18]. According to these studies, Fe (II) reduction process is reversible and diffusion-controlled [6,7,13,16] although in some cases it has shown some features which do not conform to a fully reversible process [13,16]. In two other studies, deviation from reversibility was high enough to consider the Fe (II) reduction as quasi-reversible [14,15]. Although, many studies have been done on

iron in chloride melts, it seems little attention has been paid to $FeCl_3$ behaviour and stability in these electrolytes. The existence of $FeCl_3$ has been reported in some of the studies [6,7,10,11,14,18]. However, it showed to be not very stable and was difficult to detect it [6,7,10]. But in some other studies iron (III) chloride was not detected at all [12,13,15,16]. Its absence has been attributed to instability/volatility of this compound [6]. It seems that the experimental conditions such as temperature, electrode material and composition of the melt have a great influence on $FeCl_3$ stability. At high temperature it decomposes to $FeCl_2$ and Cl_2 [19]. This reaction may be catalysed by the electrode surface [6]. In addition, the electrode itself may participate in electrochemical reactions by alloying with iron and complicating reactions [12] or through oxidation and chemically reducing Fe (III) ions; the latter conceals electrochemical oxidation of Fe (II) to Fe (III) [20]. Composition of the melt also has an important effect [21]. It has been shown that, $FeCl_3$ and likewise $AlCl_3$ [22], reacts with alkali chlorides and forms stable complexes, with the general formula of $MFeCl_4$, where M is the alkali metal [23]. The other parameter which may have a role in determining the stable ions, is the method used to introduce the iron ions into the melt. In many studies, Fe (II) ions were generated by anodic dissolution of metallic iron at constant current (coulometry) [14,10]. On the other hand, it has been reported that the addition of anhydrous $FeCl_3$ leads to generation of stable Fe (III) ions [18] while other papers have shown that $FeCl_3.6H_2O$ can serve as a source of bivalent iron [12-13]. In those two cases, where $FeCl_3$ was added to the melt [11,18], the reduction occurred in one single reversible step; Fe (III)/Fe (0). In contrast, two other studies reported that the reduction occurred in two steps and that the Fe (II)/Fe (III) exchange was either reversible [17] or quasi-reversible [14].

This work is a study of the electrochemical behaviour of iron in molten LiCl+KCl+NaCl mixture at 550ºC. In addition to basic electrochemical discussions, this study even looks at the behaviour of $FeCl_3$ based on current results and previous studies. The chosen electrolyte is used for "salt extraction process", a molten salt electrolytic process for recovery of metallic values from waste materials e.g. steel slag. This process was firstly applied to steel slag for the recovery of chromium and iron at elevated temperatures; e.g. 900ºC. The electrolyte was KCl+NaCl [20]. Later some modifications were applied to the process which enabled performing the process at lower temperatures. Therefore the electrolyte was changed to the ternary mixture of LiCl+KCl+NaCl. The ternary phase diagram shows a ternary eutectic reaction at 346ºC [25]. Therefore, this mixture has the capacity for a low temperature electrolytic process. Nevertheless, it is worth mentioning that the composition of this ternary mixture is very close to the binary KCl+LiCl, which is the common molten salt used for many similar processes.

2. Experimental

All the chemicals including KCl, LiCl, NaCl and $FeCl_3$ (Sigma Aldrige, 99 %) were weighed and kept in a glove box to avoid contact with moisture and oxygen. The required amounts of alkali metal chlorides, i.e. 52 mol% LiCl + 40 mol% KCl + 8 mol% NaCl, were mixed together. This is the composition of the eutectic point of their ternary system at 346ºC [25]. An air-tight three-electrode cell with alumina radiation shields and a glassy carbon crucible (65 mm diameter and 72.5 mm height) were used in the experiments. A flow of argon was kept during the experiments to provide an air free atmosphere; argon gas was also used for stirring the electrolyte. A 1 mm diameter tungsten wire and a 2.3 mm diameter glassy carbon rod served as working electrodes and a graphite rod (5 mm

diameter) was used as the counter electrode. A silver wire (1 mm diameter) dipped into the mixture of same electrolyte plus 10 wt% AgCl inside a pythagoras (alumina + silica) tube served as the reference electrode. The temperature was measured using a type S thermocouple (Pt-Pt/10 % Rh). The electrolyte (100 g) was heated at 200ºC and kept at this temperature overnight and then heated to 550ºC. Cyclic voltammetry and chronoamperometry were performed in order to study the iron behaviour in this electrolyte. The measurements were done using an Autolab PGStat-30 potentiostat.

3. Results and discussion

3.1. Basic electrochemical response

Figure 1 shows the voltammogram for the Fe (II) solution on glassy carbon electrode. There is one couple of cathodic and anodic current peaks between -0.9 to -0.2 V. The shapes of the peaks are typical for the formation and reoxidation of a constant activity product; the cathodic peak, marked as A, shows a break at the beginning of the reduction and the anodic peak, marked as A', is a sharp stripping peak. Considering the peak potential values, the extrema A and A' are related to the reduction of Fe (II) and stripping of deposited iron, respectively. At lower potentials the deposition of alkali metal chlorides (NaCl/LiCl) defines the cathodic end of the electrochemical window. It can be seen that the discharge of alkali metal ions (Li/Na) starts from potentials as high as -1.2 V which is much more positive than the standard value. On tungsten electrode the deposition begins at around -1.9 V [18]. It is well-known that alkali metals (especially Li) reacts with graphite and this leads to the underpotential deposition of these metals [26,27]. But, in this study the substrate was glassy carbon which is less reactive than graphite. Therefore, this shift in reduction potential is unexpected and the reason was not

identified. Nevertheless, it is not related to iron ions since the same phenomenon was observed in the pure electrolyte before adding the iron chloride. There is another couple (cathodic, B and anodic B') located between 0.4 and 1.1 V. The shape of these peaks is characteristic of a soluble-soluble exchange which can be attributed to the exchange of Fe (II)/Fe (III) ions. Continuation of anodic peak, B', connects to chlorine evolution at the other end of the electrochemical window. These conform to the results in similar studies [11,14].

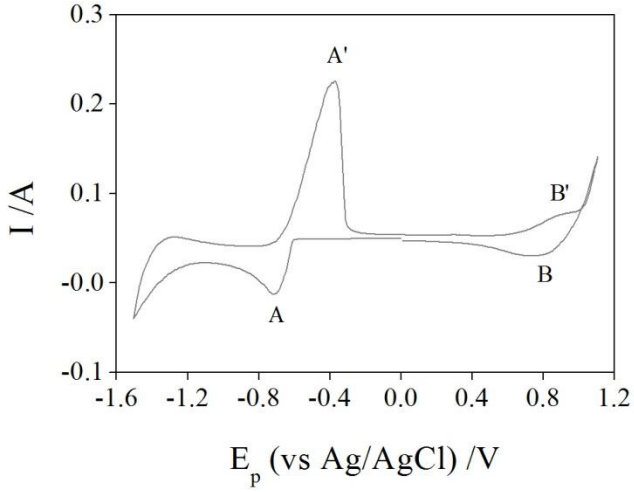

Figure 1: Linear sweep voltammogram for reduction of iron chloride obtained on glassy carbon electrode in KCl+LiCl+NaCl melt at 550ºC with sweep rate equal to 1 V s^{-1}; $FeCl_2$ concentration: $6.1*10^{-2}$ mol dm^{-3}.

3.2. Fe (II) / Fe (0) exchange

As can be seen in Figure 1 the cathodic peak corresponding to Fe (II) reduction and deposition has a steep rise and slow decay. For the anodic peak the decay is steeper than the rise which is characteristic for a stripping peak [14].

The voltammograms recorded at different sweep rates shown in Figure (a) shows that the cathodic and anodic peak potentials shift as the sweep rate is increased. Figure (b)

illustrates the variation of the cathodic peak potential with the logarithm of the sweep rate. Considering the value of $\Delta E_P^c/\Delta log v$ (= 48 mV) and also the peak separation $\Delta E_P (= E_P^c - E_P^a)$ suggest that the process is not fully reversible [28,29].

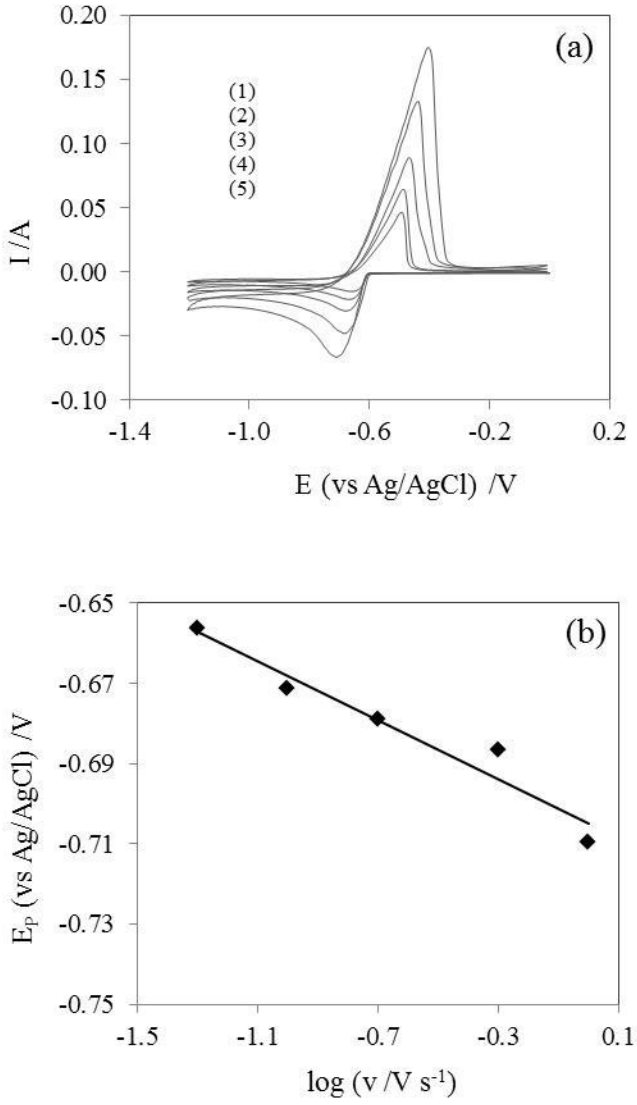

Figure 2 a) Voltammetry for Fe (II) / Fe (0) exchange at different sweep rates; (1) 1, (2) 0.5, (3) 0.2, (4) 0.1 and (5) 0.05 V s^{-1}. $FeCl_2$ concentration: $6.1*10^{-2}$ mol dm^{-3} (0.0382 mol kg^{-1}), glassy carbon electrode, electrode area: 0.4748 cm^2. b) Variation of the cathodic peak current potential with the logarithm of the sweep rate.

Figure (a) and (b) illustrate the dependency of peak current densities on concentration of Fe^{2+} and square root of scan rates, respectively. They both show a linear behaviour with intercepts almost equal to zero which suggests a diffusion-controlled process [28,29].

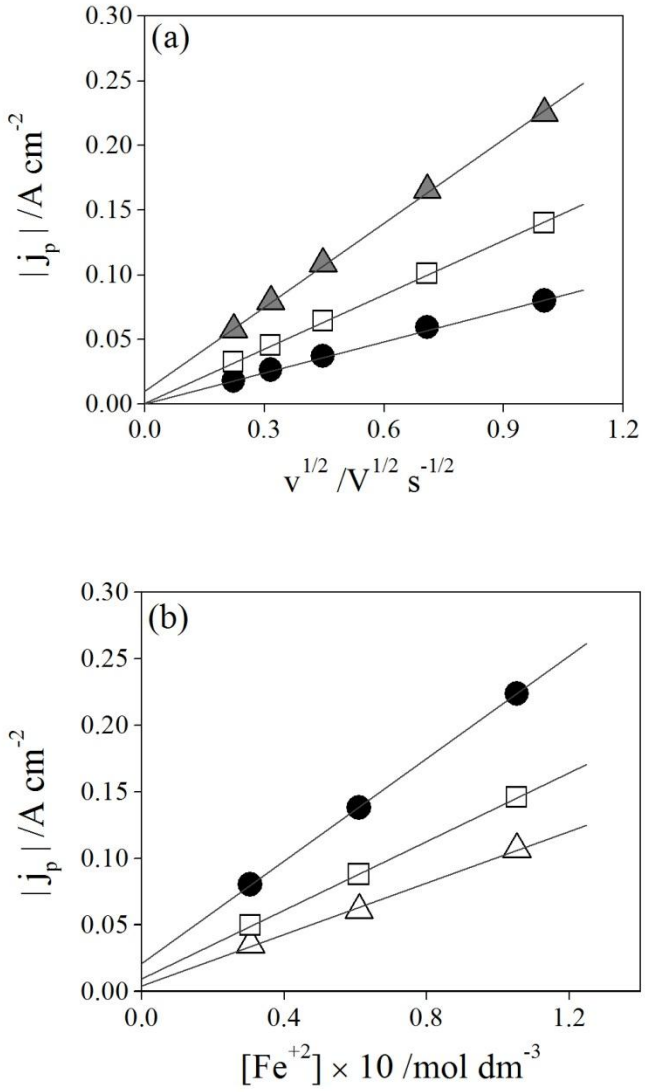

Figure 3 a) The dependence of the absolute value of the peak current density on square root of sweep rate for Fe^{2+} reduction on glassy carbon electrode in a KCl+LiCl+NaCl melt at 550ºC, different concentration of the ions. ● $3.05*10^{-2}$ mol dm^{-3} Fe^{2+}; □ $6.1*10^{-2}$ mol dm^{-3} Fe^{2+}; Δ $10.5*10^{-2}$ mol dm^{-3} Fe^{2+}. b) The dependence of the absolute value of the cathodic peak current

density on concentration of iron ion ([Fe^{+2}]) for different scan rates: ● 0.5 V s^{-1}, □ 0.2 V s^{-1}, Δ 0.1 V s^{-1}.

It is likely that the observed peak separation is due to an uncompensated resistance [28]. Besides, in Figure 3, some of the intercepts are very close to zero, but not exactly zero. These small positive values for intercepts cannot invalidate our deduction regarding that the process is diffusion-controlled. This can be attributed to the effect of iron deposition. Similar observation were reported elsewhere [13,16].

Considering all these, the Fe(II)/Fe(0) process in this study can be considered reversible and diffusion controlled. Obviously it is not fully reversible and it shows a low degree of irreversibility. This type of behaviour has been reported in other similar studies [13,16].

3.3. Electrochemical nucleation

Figure 4 (a) illustrates *I–t* transients obtained for the deposition of iron on glassy carbon. As can be seen the transient at -580 mV (curve 1) is typical for a diffusion controlled process. When the applied potential increases, the situation changes and nucleation behaviour appears in the transients. First, the current passes through a minimum which is due to the coincidence of the falling charging current with the as yet small nucleation growth current. This is followed by a maximum which has been attributed to the overlap of neighbouring diffusion zones. Finally, the current decays with time which is because the process becomes completely diffusion controlled [30]. These features can be more clearly detected in curves 4 and 5 in Figure 4 (a). The minimum and maximum currents show high sensitivity to the value of the stepped potential. This reveals that at high enough overpotential, nucleation and growth phenomena have a significant role in the

overall process. Similar behaviours have been reported for deposition of iron on glassy carbon [14] and tungsten electrodes [16].

The nucleation behaviour depends on the rate of appearance of stable growth centres. There are two limiting cases referred to as instantaneous and progressive nucleation. In instantaneous nucleation all the nuclei are created at the same moment at the beginning of the electrolysis, where in progressive nucleation new crystals are continuously created throughout electrolysis.

In order to determine the mode of nucleation behaviour in this study two analytic methods have been used: (i) the non-dimensional plots for chronoamperometric curves; and (ii) the product of $j_{max}^2 t_{max}$ where t_{max} and j_{max} respectively represent the time and current density corresponding to the maximum in each transient.

Figure 4 (b) illustrates the non-dimensional plots. As can be seen the experimental values show instantaneous nucleation which agrees with the results of another study of iron deposition on glassy carbon in $ZnCl_2$+2NaCl at 450ºC [14].

The other criterion, the product of ($j_{max}^2 t_{max}$), was also examined for potentials equal -610 and -620 mV. The value of $j_{max}^2 t_{max}$ was achieved both by calculation from the corresponding equations and also through multiplying the measured experimental values. These are represented in Table 1. From comparison of these two methods, it was ascertained that the nucleation mode is closer to the instantaneous limiting case; this conforms to the result of the first criterion as well as previous studies [14].

In the experimental data presented in Figure 4 (b) some parts exist which are out of range. This can be attributed to the effect of periodic electrical noise while the

experiment was performed. The corresponding data points can be detected in curves 4 and 5 in Figure 4 (a), where they appear as knots.

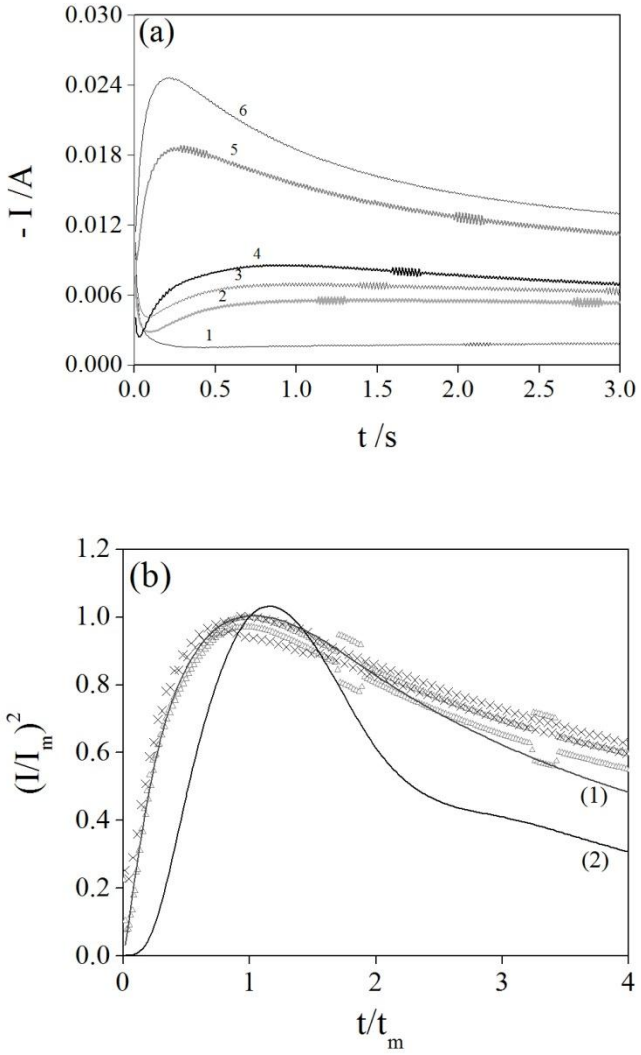

Figure 4 a) Potentiostatic current transients for electrochemical deposition of iron on glassy carbon electrode in LiCl+KCl+NaCl at 550ºC. The applied potentials are: (1) -580, (2) -590, (3) -595, (4) -600, (5) -610, and (6) -620 mV. $FeCl_2$ concentration: $1.05*10^{-1}$ mol dm^{-3}, electrode area: 0.5109 cm^2. b) Comparison of the dimensionless experimental data derived from the current-time transient with the theoretical models for (1) instantaneous and (2) progressive nucleation at different overvoltages: (X) -600, and (Δ) -610 mV vs. Ag/AgCl

Table 1 Comparison of calculated values of $j_{max}^2 t_{max}$ from equations and measured data for determining the nucleation mode

$j_{max}^2 t_{max}$ /A^2 cm^{-2} s $\times 10^5$

Calculated from the measured values		Calculated from the corresponding equations	
(Stepped potential (vs Ag/AgCl) /V)		Instantaneous	Progressive
41.3 (-0.61)	45.2 (-0.62)	66.9	106.7

3.4. Diffusion coefficient of Fe (II)

The diffusion coefficient was calculated using different electrochemical techniques. Based on cyclic voltammetry studies, this can be done from the slope of the lines in Figure 3 (a) and by using the suitable equation. One model for the electrodeposition on a solid electrode was developed by Berzins – Delahay [31]. The equation is derived based on the assumption of a constant activity of metal deposit equal to unity. This model seems to give the best description for the process of metal deposition on solid electrodes in fused salt melts [13]:

$$I_P = 0.6105nFSc(nF/RT)^{1/2}\, v^{1/2}\, D^{1/2} \qquad (1)$$

here I_P is the cathodic peak current from the voltammogram, n is the number of electrons transferred (here n = 2), F is the Faraday's constant, R is the gas constant, S is the area of the electrode (cm^2), c is the bulk concentration of Fe^{2+} (mol cm^{-3}), T is the absolute temperature, D is the diffusion coefficient ($cm^2\ s^{-1}$) and v is the scan rate (V s^{-1}). The values of the diffusion coefficient for Fe^{2+}, calculated at different concentrations, are summarized in Table 2.

The calculated values obtained here are in agreement with the previous studies [6,9,12-14,16]. As can be seen, the values of the diffusion coefficient are not clearly independent of the concentration of iron ions. They are conversely correlated to concentration. This has also been mentioned in [13] and has been attributed to the structure reorganization of the molten chloride systems.

Table 2: Diffusion coefficients of Fe^{2+} in KCl+LiCl+NaCl melt at 550°C

c/ mol dm^{-3}	$D*10^5$, cm^2 s^{-1}
0.031	1.8
0.061	1.3
0.105	1.1

3.5. Fe (III)

As can be seen in Figure 1, the oxidation potential of Fe (II) to Fe (III) is very close to that of oxidation of Cl^- ions to form chlorine gas. In addition, $FeCl_3$ is only partially stable in these melts. This make the study of this process difficult; achieving precise and clear experimental data sometimes become elusive [6,7] and interpretation of them would be difficult. In this study, current peaks related to $FeCl_3$ redox reactions were detected in voltammograms, Figure 1. In the following comes our observations and discussion. However, the necessity of a more thorough investigation on Fe (II) oxidation in chloride melts seems obvious.

The voltammograms recorded at different sweep rates are illustrated in Figure 5 (a) and the variation of the anodic peak potential with the logarithm of sweep rate is shown in Figure 5 (b). It is obvious that as the sweep rate increases the peak potentials shift which implies some irreversibility for this process [28,29]. The value of $\Delta E_P^a / \Delta log v$ is equal to 73 mV which confirms this fact. In a similar study [14] some irreversibility has been reported but our results show a higher degree of irreversibility.

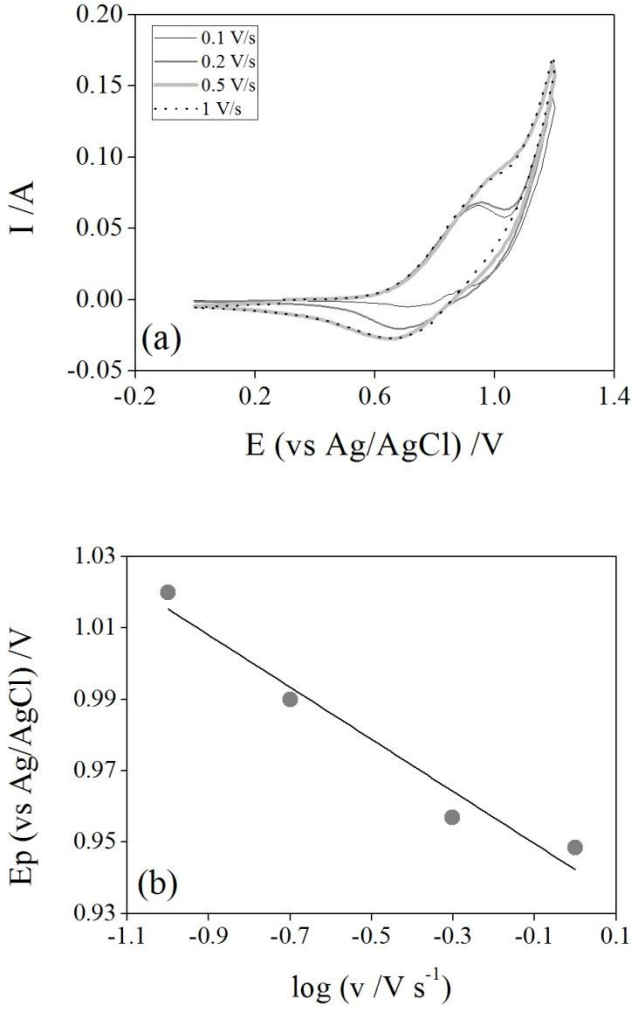

Figure 5 a) Voltammetry for the Fe (III) / Fe (II) exchange at different sweep rates; (1) 1, (2) 0.5 (dashed line), (3) 0.2, and (4) 0.1 V s^{-1}. $FeCl_2$ concentration: $1.05*10^{-1}$ mol dm^{-3} (0.0658 mol kg^{-1}), glassy carbon electrode, electrode area: 0.5109 cm^2. b) Variation of the anodic current peak potential with the logarithm of the sweep rate.

Figure 6 shows the absolute value of the peak current densities for both cathodic and anodic reactions versus square root of sweep rate. On the reverse scan the reduction current decreases considerably; but at higher scan rates the reverse peak becomes more apparent. Furthermore, at higher sweep rates the absolute value of the anodic peak current does not show a noticeable change.

These observations suggest the influence of a chemical reaction. Oxidizing Fe (II) ions on the forward scan leads to the production Fe (III) ions. Before the cathodic reaction occurs on the reverse scan, the Fe (III) ions are consumed in a chemical reaction. The $FeCl_3$ concentration in the electrolyte drops which in turn causes the cathodic current decreases on reverse scan. However at higher sweep rates, there is less time for the chemical reaction to proceed, thus, the reverse current is higher; Figure 5 (a) and Figure 6. Also, the value of $j_p^a/v^{1/2}$ decreases slightly when sweep rate is increased, which is another feature for this type of process [28]

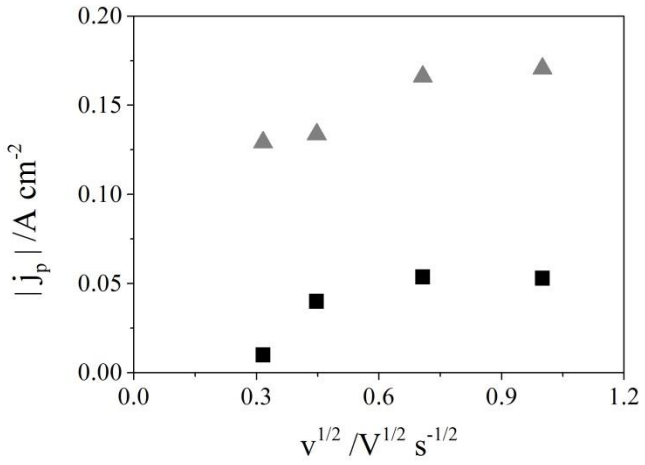

Figure 6 Dependence of the absolute value of the peak current density on the square root of the scan rate for both oxidation (Δ) and reduction (□) reactions between Fe^{2+} and Fe^{3+} on glassy carbon electrode in a KCl+LiCl+NaCl melt at 550ºC, concentration of $FeCl_2$: $1.05*10^{-1}$ mol dm^{-3} (0.0658 mol kg^{-1}).

As mentioned before, in this study the iron ions where introduced into the melt through addition of $FeCl_3$. Due to the higher stability of $FeCl_2$, the equilibrium between Fe (II) and (III) chlorides (equation 2) moves in favour of $FeCl_2$ formation.

$$FeCl_{3\,(melt)} = FeCl_{2\,(melt)} + 1/2\,Cl_{2\,(gas)} \qquad (2)$$

And the Fe (II)/Fe (0) exchange was observed, Figure 2. When the potential is shifted to more positive values the Fe (III)/Fe (II) can also be seen. This suggests that $FeCl_3$ is also present and partially stable at the experimental conditions of this study. However, anodic oxidation of Fe(II) leads to the formation of Fe(III) ions and the equilibrium of equation 2 is distorted. Therefore, the reaction moves to the right direction and before the electrochemical reduction occurs on the reverse scan, $FeCl_3$ is chemically converted to $FeCl_2$. Therefore, as much as the timescale of the scan is longer, the cathodic current on the reverse scan decreases.

Unlike the two other studies [11,18] where addition of anhydrous $FeCl_3$ resulted in a single reduction step (Fe(III)/Fe(0)), here the addition of anhydrous $FeCl_3$ to the melt led to the formation of both iron (II) and iron (III) ions. The reason for this could be the lower working temperature in the current work and also the composition of the electrolyte. It seems that the equilibrium between iron chlorides (equation 2) does not proceed until complete conversion of $FeCl_3$ to $FeCl_2$. Iron (III) chloride proves to be partially stable. This is likely because of the presence of KCl and NaCl in this melt which enhances the stability of $FeCl_3$ through formation of complexes [32]. The other significant parameter is the chlorine gas pressure. If the pressure of Cl_2 is kept very low (close to zero) $FeCl_3$ decomposes completely. On the other hand, the solubility of chlorine in these melts is low. Therefore, the equilibrium between chlorides can disrupt easily. If chlorine gas is supplied, the $FeCl_2$ formed from the decomposition of $FeCl_3$ reacts with chlorine gas and again forms $FeCl_3$ [21]. As can be seen in Figure 5, here the evolution of chlorine gas is possible; which may have influenced the equilibrium of equation 2. This may also explain the different observations that have reported upon

adding $FeCl_3$ into the chloride melts [1218]. After recording the voltammograms for the Fe (II)/Fe (III) exchange, a yellow deposit was formed on the cooler part of the cell. A similar observation has been reported elsewhere [6,11,16]. The resulting yellow deposit was analysed and identified to be $FeCl_3$ [6]. However, we did not analyse any deposits in the present work.

One important point is that the concentration of iron which is generally reported as either solely Fe (II) or Fe (III) cannot be precise, if the possibility of the exchange reaction between these ions is not considered. The concentration value, at every stage of the experiment, becomes more reliable if the experimental conditions and the consequence of experimental procedure are monitored carefully.

4. Conclusion

The electrochemical behaviour of iron was studied in the KCl+LiCl+NaCl mixture at 550ºC by cyclic voltammetry and chronoamperometry. The Fe (II)/Fe (0) exchange proves to be a soluble-insoluble diffusion controlled process, although it cannot be considered as fully reversible. Analysis of *I-t* diagrams obtained from chronoamperometry suggests an instantaneous nucleation process for metallic iron on glassy carbon electrode. The value calculated for the diffusion coefficient of Fe^{2+} 1.4×10^{-5} cm^2 s^{-1} is in agreement with previous studies. Although $FeCl_3$ is not fully stable in these types of solutions, the Fe (II)/Fe (III) exchange reaction was observed at potentials near the chlorine evolution reaction. The oxidation of Fe (II) to Fe (III) is followed by a chemical reaction consuming the as generated $FeCl_3$ ions. Analysis of the Fe (II)/Fe (III)

voltammograms suggest that the process is not reversible and is coupled with a chemical reaction.

Acknowledgement

The authors wish to express their gratitude to the financial support from the Swedish Environmental Research Foundation (Mistra project No. 88034).

References

1. W. Simka, D. Puszczyk, G. Nawrat, Electrodeposition of metals from non-aqueous solutions, Electrochimica Acta 54 (2009) 5307.
2. D. Inman, S.H. White, The production of refractory metals by electrolysis of molten salts design factors and limitations, Journal of Applied Electrochemistry 8 (1978) 375.
3. G.M. Haarberg, E. Kvalheim, S. Rolseth, T. Murakami, S. Pietrzyk, S. Wang, Electrodeposition of Iron from Molten Mixed Chloride/Fluoride Electrolytes, ECS Transactions 35 (2007) 341.
4. D. Wang, A.J. Gmitter, D.R. Sadoway, Production of oxygen gas and liquid metal by electrochemical decomposition of molten iron oxide, Journal of the Electrochemical Society, 158 (2011) 51.
5. A. Allanore, H. Lavelaine, G. Valentin, J.P. Birat, F. Lapicque, Iron Metal Production by Bulk Electrolysis of Iron Ore Particles in Aqueous Media, Journal of Electrochemical Society 155 (2008) 125.

6. D. Inman, J.C. Legey, R. Spencer, A chronopotentiometric study of iron in LiCl-KCl, Journal of Applied Electrochemistry 8 (1978) 269.

7. G. Picard, F. Seon, and B. Tremillon, Reactions of Formation and Stability of Iron (II) and (III) Oxides in LiCl-KCl Eutectic Melt at 470ºC, Journal of Electrochemical Society 129 (1982) 1450.

8. F. Seon, G. Picard, D. Tremillon, Stability of ferrous oxide in molten LiCl+KCl eutectic at 470ºC, Journal of Electroanalytical Chemistry and Interfacial Electrochemistry 138 (1982) 315.

9. J.C. Poignet, M.J. Barbier, Determination des coefficients et des enthalpies d'activation de diffusion de quelques cations dans l'eutectique LiCl-KCl fondu par chronopotentiometrie, Electrochimica Acta 17 (1972) 1227.

10. H.A. Laitinen, J.W. Pankey, Halogen, Iron and Vanadium Potentials in Lithium Chloride-Potassium Chloride Eutectic, Journal of the American Chemical Society 81 (1959) 1053.

11. X.L. Ge, S.J. Xiao, G.M. Haarberg, S. Seetharaman, Salt extraction process-novel route for metal extraction Part 3-electrochemical behaviours of metal ions (Cr, Cu, Fe, Mg, Mn) in molten ($CaCl_2$-) NaCl-KCl salt system, Transactions of the Institutions of Mining and Metallurgy, Section C: Mineral Processing and Extractive Metallurgy 119 (2010) 163.

12. A. Lugovskoy, M. Zinigrad, D. Aurbach, Z. Unger, Electrodeposition of iron(II) on platinum in chloride melts at 700–750°C, Electrochimica Acta 54 (2009) 1904.

13. A. Lugovskoy, M. Zinigrad, D. Aurbach, Electrochemical determination of diffusion coefficients of iron(II) ions in chloride melts at 700–750°C, Israel Journal of Chemistry 47 (2007) 409.

14. Y. Castrillejo, A.M. Martínez, M. Vega, E. Barrado, G. Picard, Electrochemical study of the properties of iron ions in $ZnCl_2$ + 2NaCl melt at 450°C, Journal of Electroanalytical Chemistry 397 (1995) 139.

15. Y. Castrillejo, A.M. Martínez, M. Vega, P. Sanchez Batanero, Electrochemical reduction of Fe(II) ions on different solid electrodes in fused $ZnCl_2$-2NaCl mixture, Journal of Applied Electrochemistry 26 (1996) 1279.

16. D. Shuzhen, P. Dudley, D. Inman, Voltammetric studies of iron in molten $MgCl_2$+NaCl+KCl: Part I. The reduction of Fe(II), Journal of Electroanalytical Chemistry and Interfacial Electrochemistry 142 (1982) 215.

17. L.G. Boxall, H.L. Jones, R.A. Osteryoung, Electrochemical Studies on Ag, Fe, and Cu Species in $AlCl_3$-NaCl Melts, Journal of Electrochemical Society 121 (1974) 212.

18. G.M. Haarberg, M. Keppert, Diffusion kinetics for the electrochemical reduction of Fe(III) species in molten NaCl-$FeCl_3$, ECS Transactions 16 (2009) 309.

19. Kirk-Othmer Encyclopaedia of Chemical Technology, Online version, Online ISBN: 9780471238966, DOI: 10.1002/0471238961, (2012) http://onlinelibrary.wiley.com/book/10.1002/0471238961

20. J. Chryssoulakis, J. Bouteillon, J.C. Poignet, Electrochemical behaviour of pure iron in the aluminium refining electrolyte, Journal of Applied Electrochemistry 8 (1978) 103.

21. G. Zhao, Q. Tian, S. Duan, Equilibria between ferrous and ferric chlorides in molten chloride salts, Metallurgical and Materials Transactions 21B (1990) 131.

22. F. Lantelme, H. Alexopoulos, M. Chemla, O. Haas, Thermodynamic properties of aluminium chloride solutions in the molten LiCl-KCl system, Electrochimca Acta 33 (1988) 761.

23. C.M. Cook, W.E. Dunn, The reaction of ferric chloride with sodium and potassium chlorides, Journal of Physical Chemistry 65 (1961) 1505.

24. X.L. Ge, O. Grinder, S. Seetharaman, The salt extraction process: a novel route for metal extraction Part I – Cr, Fe recovery from EAF slags and low grade chromite ores, Transactions of the Institutions of Mining and Metallurgy, Section C: Mineral Processing and Extractive Metallurgy 119 (2010) 27.

25. E.M. Levin, C.R. Robbins, H.F. McMurdie, Phase diagrams for ceramics vol. III, The American Ceramic Society, 1969.

26. N. Adhoum, J. Bouteillon, D. Dumas, J.C. Poignet, Electrochemical insertion of sodium into graphite in molten sodium fluoride at 1025ºC, Electrochimica Acta 51 (2006) 5402.

27. Q. Xu, C. Schwandt, D.J. Fray, Electrochemical investigation of lithium intercalation into graphite from molten lithium chloride, Journal of Electroanalytical Chemistry 530 (2002) 16.

28. Southampton Electrochemistry Group, Instrumental Methods in Electrochemistry, Woodhead publishing, Cambridge, 1985.

29. A.J. Bard, L.R. Faulkner, Electrochemical Methods: Fundamentals and Applications, John Wiley & Sons, New York, 1980.

30. G. Gunawardena, G. Hills, I. Montenegro, B. Scharifker, Electrochemical nucleation: Part I. General considerations, Journal of Electroanalytical Chemistry and Interfacial Electrochemistry 138 (1982) 225.

31. T. Berzins, P. Delahay, Oscillographic Polarographic Waves for the Reversible Deposition of Metals on Solid Electrodes, Journal of the American Chemical Society 75 (1953) 555.

32. J. Iwanec, B.J. Welch, The removal of dissolved iron chlorides from molten chloride mixture, Australian Journal of Chemistry 22 (1969) 1783.

Captions:

Figure 1: Linear sweep voltammogram for reduction of iron chloride obtained on glassy carbon electrode in KCl+LiCl+NaCl melt at 550ºC with sweep rate equal to 1 V s^{-1}; $FeCl_2$ concentration: $6.1*10^{-2}$ mol dm^{-3}.

Figure 2: a) Voltammetry for Fe (II) / Fe (0) exchange at different sweep rates; (1) 1, (2) 0.5, (3) 0.2, (4) 0.1 and (5) 0.05 V s^{-1}. $FeCl_2$ concentration: $6.1*10^{-2}$ mol dm^{-3} (0.0382 mol kg^{-1}), glassy carbon electrode, electrode area: 0.4748 cm^2. b) Variation of the cathodic peak current potential with the logarithm of the sweep rate.

Figure 3: a) The dependence of the absolute value of the peak current density on square root of sweep rate for Fe^{2+} reduction on glassy carbon electrode in a KCl+LiCl+NaCl melt at 550ºC, different concentration of the ions. ● $3.05*10^{-2}$ mol dm^{-3} Fe^{2+}; □ $6.1*10^{-2}$ mol dm^{-3} Fe^{2+}; Δ $10.5*10^{-2}$ mol dm^{-3} Fe^{2+}. b) The dependence of the absolute value of the cathodic peak current density on concentration of iron ion ($[Fe^{+2}]$) for different scan rates: ● 0.5 V s^{-1}, □ 0.2 V s^{-1}, Δ 0.1 V s^{-1}.

Figure 4: a) Potentiostatic current transients for electrochemical deposition of iron on glassy carbon electrode in LiCl+KCl+NaCl at 550ºC. The applied potentials are: (1) -580, (2) -590, (3) -595, (4) -600, (5) -610, and (6) -620 mV. $FeCl_2$ concentration: $1.05*10^{-1}$ mol dm^{-3}, electrode area: 0.5109 cm^2. b) Comparison of the dimensionless experimental data derived from the current-time transient with the theoretical models for (1) instantaneous and (2) progressive nucleation at different overvoltages: (X) -600, and (Δ) -610 mV vs. Ag/AgCl.

Figure 5: a) Voltammetry for the Fe (III) / Fe (II) exchange at different sweep rates; (1) 1, (2) 0.5 (dashed line), (3) 0.2, and (4) 0.1 V s^{-1}. $FeCl_2$ concentration: $1.05*10^{-1}$ mol dm^{-3} (0.0658 mol kg^{-1}), glassy carbon electrode, electrode area: 0.5109 cm^2. b) Variation of the anodic current peak potential with the logarithm of the sweep rate.

Figure 6: Dependence of the absolute value of the peak current density on the square root of the scan rate for both oxidation (Δ) and reduction (□) reactions between Fe^{2+} and Fe^{3+} on glassy carbon electrode in a KCl+LiCl+NaCl melt at 550ºC, concentration of $FeCl_2$: $1.05*10^{-1}$ mol dm^{-3} (0.0658 mol kg^{-1}).